Available online at www.sciencedirect.com
SCIENCE DIRECT®
Bioorganic & Medicinal Chemistry Letters 16 (2006) 3514–3518
Bioorganic & Medicinal Chemistry Letters

Development of *N*-2,4-pyrimidine-*N*-phenyl-*N*′-alkyl ureas as orally active inhibitors of tumor necrosis factor alpha (TNF-α) synthesis. Part 2

Jennifer A. Maier, Todd A. Brugel,* Michael P. Clark, Mark Sabat, Adam Golebiowski, Roger G. Bookland, Matthew J. Laufersweiler, Steven K. Laughlin, John C. VanRens, Biswanath De, Lily C. Hsieh, Kimberly K. Brown, Karen Juergens, Richard L. Walter and Michael J. Janusz

Procter & Gamble Pharmaceuticals, Health Care Research Center, 8700 Mason-Montgomery Rd., Mason, OH 45040, USA

Received 10 March 2006; revised 27 March 2006; accepted 28 March 2006
Available online 24 April 2006

Abstract—A new class of tumor necrosis factor alpha (TNF-α) synthesis inhibitors based on a *N*-2,4-pyrimidine-*N*-phenyl-*N*′-alkyl urea scaffold is described. Many of these compounds showed low-nanomolar activity against lipopolysaccharide stimulated TNF-α production. Two analogs were tested in an in vivo rat iodoacetate model of osteoarthritis and shown to be orally efficacious. X-ray co-crystallization studies with mutated p38α showed that these trisubstituted ureas interact with the ATP-binding pocket in a pseudo-bicyclic conformation brought about by the presence of an intramolecular hydrogen bonding interaction.

The over-expression of cytokines, such as tumor necrosis factor alpha (TNF-α) and interleukin-1β (IL-1β), has been implicated in a number of serious inflammatory disorders.[1] Consequently, agents that inhibit the proliferation of these pro-inflammatory cytokines could reduce inflammation and prevent further tissue destruction in diseases such as rheumatoid arthritis (RA),[2], osteoarthritis (OA) and Crohn's disease.[3] When activated by external stimuli, the serine-threonine kinase p38 mitogen-activated protein (MAP) kinase perpetuates a phosphorylation cascade among downstream kinases which activates transcription factors such as NF-κβ leading to ultimate synthesis of TNF-α and IL-1β.[4,5] Many companies have developed small molecule TNF-α production inhibitors that function by competitively binding to the ATP-binding pocket of p38.[6] A recent review stated that since 1996, over 234 patents have been published claiming p38 inhibitors, while seventeen specific inhibitors have been selected for development.[7] A summary of the clinical development of five recent candidates (AMG 548, BIRB 796, SCIO 469, SCIO 323, and VX 702) was recently published.[8] To date, no company has reported results for a p38 specific kinase inhibitor past phase II development.

Previously we reported the synthesis and biological activity of a series of bicyclic pyrazolone-based inhibitors of TNF-α production exemplified by **1** (TNF-α IC_{50} = 22 nM, Fig. 1) which was orally active in an

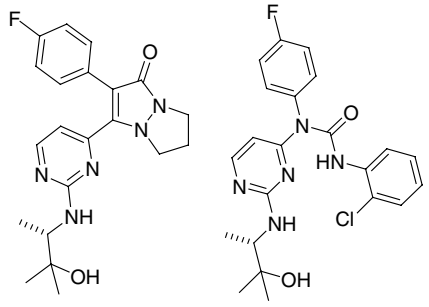

Figure 1. Urea-based pro-inflammatory cytokine inhibitor.

Keywords: Cytokine synthesis inhibitors; p38α kinase; Urea.
* Corresponding author. Tel.: +1 513 622 4498; fax: +1 513 622 3681; e-mail: brugel.ta@pg.com

0960-894X/$ - see front matter © 2006 Elsevier Ltd. All rights reserved.
doi:10.1016/j.bmcl.2006.03.096

in vivo model for osteoarthritis.[9] Pyrazolone **1** was also a potent inhibitor of p38α (IC_{50} = 54 nM), while showing a good overall profile of kinase selectivity. We followed this work with an investigation of an *N*-2,4-pyrimidine-*N*,*N*′-diphenyl urea scaffold highlighted by the potent TNF-α synthesis inhibitor **2**.[10] However, due to issues with chemical stability, we were unable to progress compounds of this class any further into in vivo studies. We now wish to report the development of new trisubstituted urea analogs which maintain cytokine inhibition, while also showing in vivo efficacy.

Synthesis of many of the described pyrimidine-ureas was accomplished in three steps from known starting materials (see Scheme 1) as reported in the previous communication.[10] Regioselective addition of 4-fluoroanilines to 2,4-dichloropyrimidine **3** gave the corresponding 6-anilino-4-chloropyrimidine **4**. A second nucleophilic addition of (3*S*)-3-amino-2-methyl-butan-2-ol to **4** in *N*-methyl pyrolidinone (NMP, 135 °C) gave the desired disubstituted pyrimidine **5**. Reaction of **5** with 2-chlorobenzyl isocyanate in dichloroethane (DCE) gave the corresponding trisubstituted ureas **6a**.[11]

The urea analogs synthesized in this study were all tested for inhibition of TNF-α in an LPS stimulated human monocytic (THP-1) whole cell-based assay.[12]

Table 1 describes the general SAR among the *N*′-benzyl-substituted urea analogs. *N*′-2-Chlorobenzyl analog **6a** was tested in the cellular assay and showed excellent potency (IC_{50} = 14 nM). This represents a near 10-fold improvement in potency over the related *N*′-2-chlorophenyl analog **2** (IC_{50} = 122 nM) described previously.[10] Additionally, unlike the corresponding *N*′-2-chlorophenyl analog **2**, the benzyl analog proved to be chemically stable in solution with no decomposition observed after 24 h standing in aqueous buffers between pH 3 and 12. Presumably, this is due to the presence of an electron-donating substituent at the N′-position which deactivates the urea toward hydrolysis relative to the *N*′-aryl

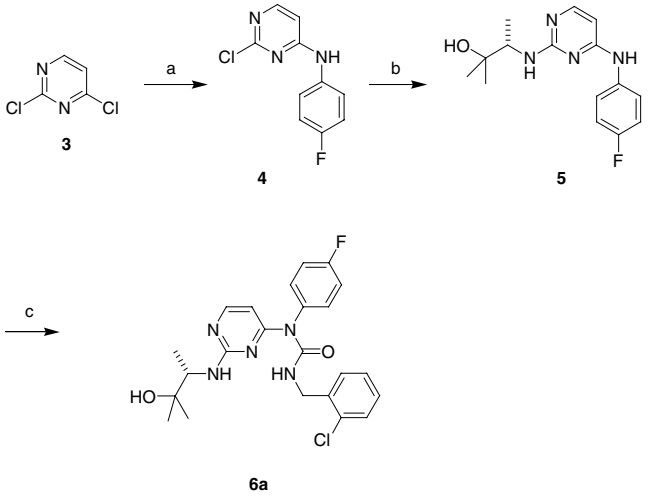

Scheme 1. Reagents and conditions: (a) EtOH, Na_2CO_3, 4-fluoroaniline; (b) NMP, *i*-Pr_2NEt, (3*S*)-3-amino-2-methyl-butan-2-ol·HCl, 135 °C; (c) DCE, 2-chlorobenzyl isocyanate, rt to 80 °C.

Table 1. TNF-α data for urea analogs containing an N′-substituted benzyl group

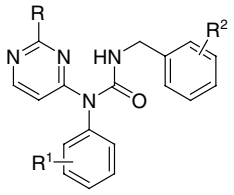

Compound	R	R^1	R^2	TNF-α IC_{50}[a] (μM)
6a	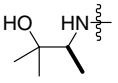	4-F	2-Cl	0.014
6b	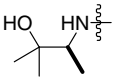	4-MeO	2-Cl	0.009
6c	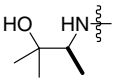	4-MeO	2-Me	0.037
6d	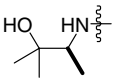	4-MeO	2-MeO	0.015
6e	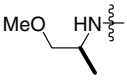	4-F	2-Cl	0.236
6f	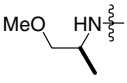	4-MeO	2-Cl	0.148
6g	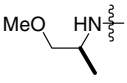	4-EtO	2-Cl	0.056
6h	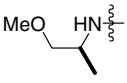	4-MeO	2,4-di-Cl	0.611
6i	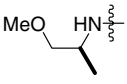	4-MeO	3,4-di-Cl	2.07
6j	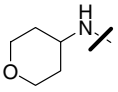	4-F	2-Cl	0.016
6k		4-MeO	2-Cl	0.016
6l	Me_2N	4-F	2-Cl	35%[b]
6m	MeNH	4-MeO	2-Cl	3%[b]
6n	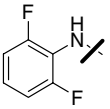	4-F	2-Cl	25%[b]

[a] Standard deviation for the assay was ±30% of mean or less.
[b] Percentage inhibition at 10 μM.

analogs. Other N′-2-substituted benzyl analogs containing the hydroxyl-dimethylpropylamino 2-pyrimidyl groups and an *N*-4-methoxyphenyl group (**6b**–**6d**) were synthesized and proved to be nearly equipotent with **6a**.

As with the *N*′-phenyl analogs, an approximate 10-fold loss in potency was observed with compounds in which

the hydroxy-dimethylpropylamino group was replaced with the methoxypropylamino group (**6e** and **6f**). The one exception in this series was the analog containing an *N*-4-ethoxyphenyl group (**6g**) which proved to be distinctly active with an IC_{50} of 56 nM. Two disubstituted benzyl derivatives were made with the 2,4-dichlorobenzyl analog **6h** showing greater potency than the 3,4-dichlorobenzyl counterpart **6i**, although both were significantly less potent than the most active analogs in the series. However, the 2-pyrimidyl tetrahydro-pyranylamino analog **6j** and isopropylamino analog **6k** proved to be the most active, non-chiral urea analogs synthesized to this point. Conversely, other 2-pyrimidyl derivatives such as the dimethylamino analog **6l**, the methylamino analog **6m**, and the 2,6-difluoroaniline derivative **6n** showed negligible activity. This reiterated the need for alkyl branching alpha to the amino linker.

Based on the success of adding an alkyl linker between *N*′-urea nitrogen and the phenyl side chain, we decided to also investigate purely *N*′-alkyl derivatives. Table 2 lists the results for a variety of simple *N*′-alkyl ureas. The alkyl urea **7a** proved to be as potent as the corresponding benzyl analog **6b**. Use of a longer chain or cyclic alkyl (**7b** and **7c**, respectively) resulted in compounds with reduced potency. Likewise, switching from hydroxy dimethylamino to methoxy propylamino also led to a significant loss in potency as evidenced by the comparison between **7d** and **7a**. However, changing to a 4-ethoxyphenyl group (**7e**) resulted in recovery of activity. The non-chiral amino analogs **7f** and **7g** containing the ethyl urea were also found to maintain decent potency relative to the most active chiral amino derivatives. Finally, the di-isopropyl amino analog **7h** showed comparable activity to **7g**, suggesting that some alkyl branching off the N′-position was well tolerated.

For more structurally diverse ureas, a modified synthetic protocol was developed (Scheme 2). For example, the appropriate disubstituted pyrimidine **8** could be reacted with *p*-nitrophenylchloroformate to give the activated carbamate **9**. Treatment of **9** with 4-aminomethylpyridine gave urea **10a**.

N′-Pyrimidyl ureas **10a** and **10b** (Table 3) were highly potent, with the 4-substituted analog being more active than the corresponding 2-substituted derivative. The ethyl-Boc-piperazine and methyl-Boc-piperidine analogs **10c** and **10d** showed reduced activity. However, removal of the Boc protecting group from these compounds gave analogs **10e** and **10f** which showed improved activity versus their protected precursors. The methyl piperidine **10f** (IC_{50} = 16 nM) was nearly equipotent with the related unsaturated analog **10a** (IC_{50} = 4 nM).

Having achieved our goal for this series of attaining excellent activity in the in vitro cell-based assay for inhibition of TNF-α production, we turned our attention to evaluating several analogs for their pharmacokinetic properties as well as in vivo efficacy. The results of these studies on three analogs are summarized in Table 4. The

Table 2. TNF-α data for urea analogs containing *N*′-alkyl substituents

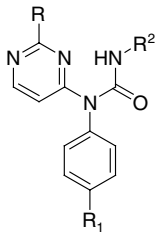

Compound	R	R^1	R^2	TNF-α IC_{50}[a] (μM)
7a	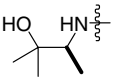	MeO	Et	0.028
7b	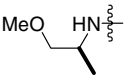	MeO	*n*-Bu	0.324
7c	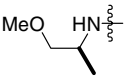	MeO	*c*-hex	0.467
7d	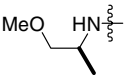	MeO	Et	0.819
7e	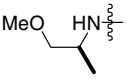	EtO	Et	0.276
7f	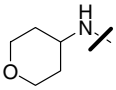	F	Et	0.086
7g		MeO	Et	0.080
7h		F	*i*-Pr	0.074

[a] Standard deviation for the assay was ±30% of mean or less.

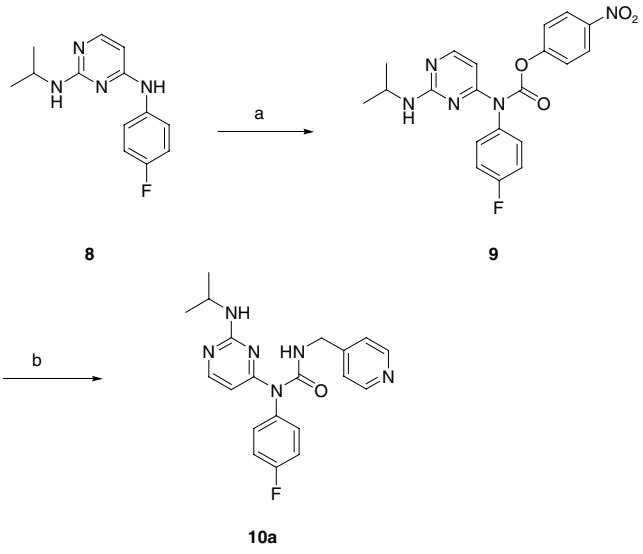

Scheme 2. Reagents and condition: (a) *p*-nitrophenylchloroformate, pyridine, CH_2Cl_2, rt; (b) 4-aminomethylpyridine, CH_2Cl_2.

Table 3. TNF-α data for urea analogs containing a 2-pyrimidyl isopropylamino substituent

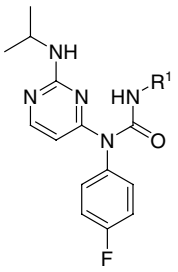

Compound	R^1	TNF-α IC_{50}[a] (μM)
10a	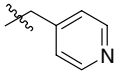	0.004
10b	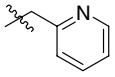	0.030
10c	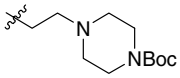	0.277
10d	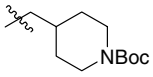	1.16
10e	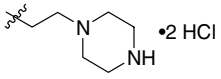	0.119
10f	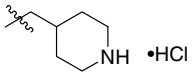	0.016

[a] Standard deviation for the assay was ±30% of mean or less.

N′-chlorobenzyl analog **6b** showed low in vitro metabolism in plated rat hepatocytes, however the low solubility and poor bioavailability prohibited us from advancing this compound further into in vivo efficacy studies. *N*′-Ethyl analogs **7a** showed low metabolism, good solubility, and acceptable bioavailability. When the chiral amino alcohol substituent in **7a** was replaced with the achiral amino tetrahydropyran group to give **7f**, the resulting analog showed an overall reduction in the described pharmacokinetic parameters. Both of these analogs showed statistically significant reduction of cartilage degradation severity compared to control in an in vivo rat iodoacetate model (25 mg/kg BID dosing) for osteoarthritis.[19,21]

Table 4. Pharmacokinetic and in vivo data for selected urea analogs

Compound	Metabolism[a] (%)	Solubility (mg/mL)	$T_{1/2}$ (h)	F (%)	Cartilage damage reduction[b] (%)
6b	32	<0.01	1.9	1.9	ND[c]
7a	32	0.24	ND	15–30[d]	24
7f	16	0.025	0.46	13.2	16

[a] Metabolism was measured as percent loss of compound after 4 h exposure to plated rat (Sprague–Dawley) hepatocytes.
[b] Reduction in severity of cartilage damage was measured versus vehicle treated animals in a rat (male Sprague–Dawley) iodoacetate (IA) model for osteoarthritis at a dose of 25 mg/kg BID ($P < 0.05$).
[c] Not determined.
[d] Estimated bioavailability based on single po dose.

An X-ray crystal structure was obtained and solved for the co-crystal formed between the *N*′-2-chlorobenzyl inhibitor **7b** and mutated p38α to obtain additional information concerning the possible mechanism for the observed TNF-α inhibition for these compounds.[15] This urea analog made many of the necessary interactions for classical p38 inhibitors (Fig. 2). Primary among these was the hydrogen bonding motif between the 2-aminopyrimidine functionality of the inhibitor and the Met-109 residue of the hinge region of the ATP-binding pocket. Additionally, the 4-methoxyphenyl group positions itself into the well-defined hydrophobic pocket defined by the 'gatekeeper' Thr-106 residue. As with the previously described phenyl urea **2**, the conformation of the urea allows for the *N*′-urea NH to form an intramolecular hydrogen bond with *N*-3 of the pyrimidine ring (2.69 Å N–N distance). This interaction created a pseudo-bicyclic arrangement for this compound, which adds rigidity to the class of inhibitors. Unlike *N*′-phenyl urea **2**, the *N*′-benzyl urea carbonyl group did form a direct hydrogen bond to Lys-53. This mimics the interaction observed for the previously described pyrazolone **1** (see molecular overlay in Fig. 2). The 2-chlorobenzyl group was positioned toward the exposed solvent pocket of the enzyme.

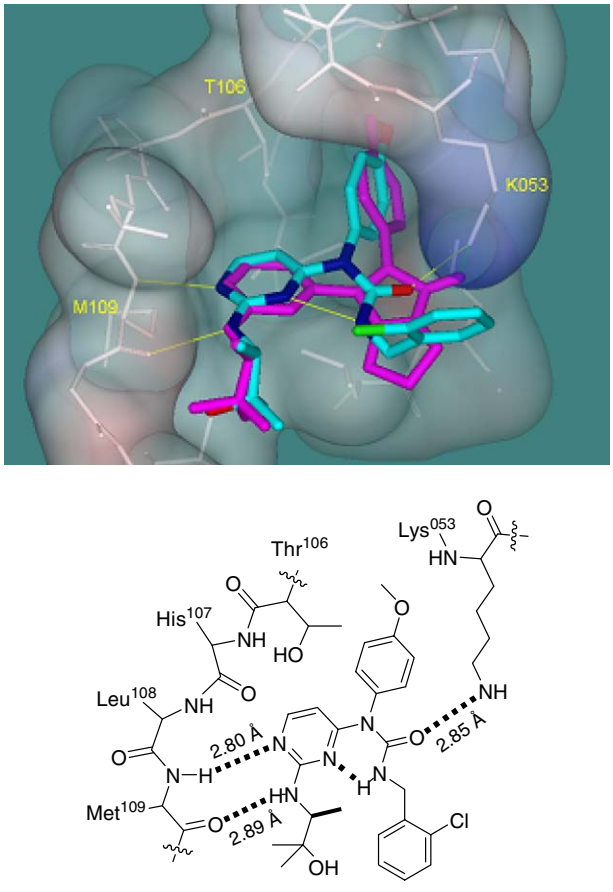

Figure 2. Co-crystal X-ray structure of **6b** (cyan) bound to mutated p38 with overlay of pyrazolone **1** (magenta).

We have developed a new class of trisubstituted ureas as inhibitors of TNF-α production. First generation *N*′-phenyl ureas, although showing good potency for inhibition of TNF-α, proved to be chemically unstable. Through development of *N*′-benzyl and alkyl urea analogs, high levels of cytokine inhibition were maintained, while achieving good chemical and metabolic stability. Several of these analogs showed good solubility and bioavailability resulting in two analogs, **7a** and **7f**, showing oral efficacy in a rat iodoacetate model for osteoarthritis. X-ray crystallography studies with mutated p38 showed a mode of binding for this class of urea inhibitors that mimics that of traditional vicinal bis-aryl MAP kinase inhibitors. Selected analogs from this class of TNF-α production inhibitors are being further developed and optimized for use as a potential treatment for various inflammatory disorders.

Acknowledgments

We are grateful to A. L. Roe, C. A. Cruze, W. E. Schwecke, and C. R. Dietsch for pharmacokinetic studies, M. Buchalova for chemical stability and solubility studies, and M. Mekel for X-ray co-crystallization studies. We thank A. G. Evdokimov and M. E. Pokross for cloning, expression, and purification of mp38 protein. We would like to acknowledge that X-ray data were collected at Southeast Regional Collaborative Access Team (SER-CAT) 22-ID (or 22-BM) beamline at the Advanced Photon Source, Argonne National Laboratory. Supporting institutions may be found at www.ser-cat.org/members.html. Use of the Advanced Photon Source was supported by the US Department of Energy, Office of Science, Office of Basic Energy Sciences, under Contract No. W-31-109-Eng-38.

References and notes

1. For a recent review, see: Adams, J. L.; Badger, A. M.; Kumar, S.; Lee, J. C. In *Progress in Medicinal Chemistry*; King, F. D., Oxford, A. W., Eds.; Elsevier: Amsterdam, 2001; Vol. 39, pp 1–60.
2. Paleolog, E. *Expert Opin. Investig. Drugs* **2003**, *12*, 1087.
3. Baugh, J. A.; Bucala, R. *Curr. Opin. Drug Discov. Devel.* **2001**, *4*, 635.
4. Herlaar, E.; Brown, Z. *Mol. Med. Today* **1999**, *5*, 439.
5. Ono, K.; Han, J. *Cell. Signalling* **2000**, *12*, 1.
6. Bolós, J. *Mini-Rev. Med. Chem.* **2005**, *5*, 857.
7. Goldstein, D. J.; Gabriel, T. *Curr. Top. Med. Chem.* **2005**, *5*, 1017.
8. Lee, M. R.; Dominquez, C. *Curr. Med. Chem.* **2005**, *12*, 2979.
9. Clark, M. P.; Laughlin, S. K.; Laufersweiler, M. J.; Bookland, R. G.; Brugel, T. A.; Golebiowski, A.; Sabat, M.; Townes, J. A.; VanRens, J. C.; Djung, J. F.; Natchus, M. G.; De, B.; Hsieh, L. C.; Xu, S. C.; Walter, R. L.; Mekel, M. J.; Heitmeyer, S. A.; Brown, K. K.; Juergens, K.; Taiwo, Y. O.; Janusz, M. J. *J. Med. Chem.* **2004**, *47*, 2724.
10. Brugel, T. A.; Maier, J. A.; Clark, M. P.; Sabat, M.; Golebiowski, A.; Bookland, R. G.; Laufersweiler, M. J., Laughline, S. K., VanRens, J. C.; De, B.; Hsieh, L. C.; Mekel, M. J.; Janusz, M. J.; *Bioorg. Med. Chem. Lett.* **2006**, in press, doi:10.1016/j.bmcl.2006.03.095.
11. All final compounds were characterized by ^{1}H NMR, HRMS, and HPLC analysis. Purity was assessed as >95%.
12. Duplicate cultures of human monocytic cells (THP-1)[13] (2.0×10^5/well) were incubated for 15 min in the presence or absence of various concentrations of inhibitor before the stimulation of cytokine release by the addition of lipopolysaccharide (final LPS concentration, 1 μg/mL). The amount of TNF-α released was measured 4 h later using an ELISA (R&D Systems, Minneapolis, MN). The viability of the cells after the 4 h incubation was measured using MTS assay[14] (Promega Co., Madison, WI).
13. Mohler, K. M.; Sleath, P. R.; Fitzner, J. N.; Cerretti, D. P.; Alderson, M.; Kerwar, S. S.; Torrance, D. S.; Otten-Evans, C.; Greenstreet, T.; Weerawarna, K.; Kronhelm, S. R.; Petersen, M.; Gerhart, M.; Kozlosky, C. J.; March, C. J.; Black, R. A. *Nature* **1994**, *370*, 218.
14. Barltrop, J. A.; Owen, T. C.; Cory, A. H.; Cory, J. G. *Bioorg. Med. Chem. Lett.* **1991**, *1*, 611.
15. The X-ray coordinates have been deposited with the Protein Data Bank, www.rcsb.org, as entry 2GHM. Mutated p38 cocrystallization/X-ray crystallography was conducted as follows: the mutated p38α herein described is a double mutant (S180A, Y182F) of murine p38α.[16] The mutant enzyme cannot be phosphorylated and, therefore, it is not competent for activation. Protein expression and purification were carried out as previously described for the murine enzyme.[17] For crystallization, mutated p38α was incubated overnight (12–16 h) with 1 mM compound. Cocrystals were grown by hanging drop vapor diffusion using PEG as a precipitating agent and overall protocols similar to those previously described for the human enzyme.[18] Crystals typically diffracted to 1.9 Å resolution and were of the previously reported space group: P212121; $a = 65.2$ Å, $b = 74.6$ Å, $c = 78.1$ Å (4′).
16. Han, J.; Lee, J. D.; Bibbs, L.; Ulevitch, R. J. *Science* **1994**, *265*, 808.
17. Wang, Z.; Harkins, P. C.; Ulevitch, R. J.; Han, J.; Cobb, M. H.; Goldsmith, E. J. *Proc. Natl. Acad. Sci. U.S.A.* **1997**, *94*, 2327.
18. Pav, S.; Whit, D. M.; Rogers, S.; Crane, K. M.; Cywin, C. L.; Davidson, W.; Hopkins, J.; Brown, M. L.; Pargellis, C. A.; Tong, L. *Protein Sci.* **1997**, *6*, 242.
19. Sprague–Dawley male rats (200–225 g) from Harlan (Oregon, WI) under anesthesia were injected in the patellar ligament region of the left leg (flexed 90° at the knee) with 20 μL of a 10 mg/mL concentration of monosodium iodoacetate (IA) (Aldrich Chemical, Milwaukee, WI). Animals (groups of 15) were dosed for 7 days BID (∼every 12 h) with the potential inhibitor (25 mg/kg) or Vehicle (2.5 mL/kg). Animals were sacrificed on day 22 and the left joint was disarticulated and fixed in 10% formalin for 24–48 h prior to capturing the image. An image of the tibial cartilage surface was captured using an Optimas (Optimas, Media Cybernetics LP, Silver Springs, MA) image analysis system. Three independent observers assessed the damage in a blinded manner using a scale of 0–4 of increasing severity (0 = normal; 4 = maximum severity).[20]
20. Guingamp, C.; Gegout-Pottie, P.; Philippe, L.; Terlain, B.; Netter, P.; Gillet, P. *Arthritis Rheum.* **1997**, *40*, 1670.
21. Janusz, M. J.; Hookfin, E. B.; Heitmeyer, S. A.; Woessner, J. F.; Freemont, A. J.; Hoyland, J. A.; Brown, K. K.; Hsieh, L. C.; Almstead, N. G.; De, B.; Natchus, M. G.; Pikul, S.; Taiwo, Y. O. *Osteoarthritis Cartilage* **2001**, *9*, 751.